Advances in Computer Science Research, volume 93
2nd International Conference on Mathematics, Modeling and Simulation Technologies and Applications (MMSTA 2019)

Numerical Simulation Study on Casing Strength of Underground Gas Storage and an Optimization Method of Casing

Guangming Zhang[1,2,*], Juan Jin[1,2], Wei Cheng[1,2], Xiaowen Zhang[1,2], Jiandong Liu[1,2], Weidong Jiang[1,2] and Luhe Shen[1,2]

[1]Research Institute of Petroleum Exploration & Development, PetroChina, Beijing 100083, China
[2]Key Laboratory of Oil & Gas Production, CNPC, Beijing 100083, China
[*]Corresponding author

***Abstract*—The casing of underground gas storage is under complex stress conditions because of the injection-production alternating loads and the influence coming from the intensive injection and withdrawal of injection-production wells. It is crucial for the long-term safety of injection-production wells of underground gas storage to conduct casing optimization and to decrease casing stress. A three-dimensional parametric finite element model of injection-production well of underground gas storage was built by employing the finite element software ABAQUS and the PYTHON scripting language. The whole process of model building was recorded by the PYTHON scripting language. It is very easy to automatically build a different model by editing and running the PYTHON script file. The model includes casing, cement sheath and formation. The spiral perforation completion was conducted in the model. The injection-production process was simulated by adopting the data coming from a field injection-production well of underground gas storage. The temporal and spatial distribution of von Mises stresses of the model was obtained from the simulation results. In order to check if the casing stress can meet relevant safety requirements, the von Mises stress of the casing was checked by employing the fourth stress strength criterion. A study on the influence of the model parameters was carried out by changing the parameters one by one, as a result of which the optimal structure and dimensions of the casing were obtained.**

Keywords—gas storage; injection-production well; casing; alternating load; optimization; finite element; numerical simulation

I. INTRODUCTION

An injection-production well of underground gas storage features intensive injection and withdrawal as well as the frequent alternation between injection and withdrawal. Due to the alternating injection and withdrawal pressures, the stresses on casing are also alternating. In addition, the casing is subject to the effect of perforations, cement sheath, formation and gas injection-production temperatures, and local stress concentration may be formed. When the local stress value exceeds the yield strength of casing steel, the casing will be damaged, bringing hidden trouble to the safe operation of gas storage. At present, there is no method or means available to evaluate casing strength and predict casing deformation for the injection-production wells of gas storage under alternating loads both at home and abroad. Therefore, it is necessary to study the casing stress and deformation trend for the injection-production wells of gas storage under alternating loads, analyze the influence of casing dimensions and structure on casing stress, and develop a casing optimization design method and technology to ensure the long-term safe and stable operation of injection-production wells of underground gas storage.

The casing of underground gas storage is under complex stress conditions. Neither theoretical analysis nor lab test can meet the requirements of actual production. Comparatively, numerical simulation is an effective method for the stress analysis and strength check of casing. In recent years, domestic and oversea scholars have applied numerical simulation to analyzing and calculating the casing stresses of injection-production wells for different types of gas storage[1-8]. However, their models are relatively simple, with no impact of the spiral perforation taken into account, nor the optimization analysis of casing structure and dimensions conducted. And most of them use tetrahedron to divide the grid freely, leaving the calculation accuracy to be further improved.

II. MATHEMATICAL-MECHANICAL EQUATIONS

A. Fluid-Solid Coupling Equations of Porous Medium

Three-dimensional fluid-solid coupling element of porous medium is used to simulate the mechanical behavior of formation rock. The porous medium of rock obeys the principle of effective stress. The stress balance equation of the porous medium of rock is expressed by the principle of virtual work, i.e. its virtual strain energy is equal to the sum of the virtual work generated by the volume force and the surface force acting on the porous medium[9].

$$\int_V \delta\dot{\boldsymbol{\varepsilon}}^{\mathrm{T}}(\overline{\boldsymbol{\sigma}} - p_m \boldsymbol{m})\mathrm{d}V = \int_S \delta\boldsymbol{v}^{\mathrm{T}}\boldsymbol{t}\mathrm{d}S + \int_V \delta\boldsymbol{v}^{\mathrm{T}}\boldsymbol{f}\mathrm{d}V \tag{1}$$

where $\delta\dot{\boldsymbol{\varepsilon}}$ is virtual strain rate matrix, s^{-1}; $\overline{\boldsymbol{\sigma}}$ is effective stress matrix, Pa; p_m is pore pressure, Pa; $\boldsymbol{m} = [1,1,1,0,0,0]^{\mathrm{T}}$; $\delta\boldsymbol{v}$ is virtual velocity vector, m/s; $\boldsymbol{t}$ is surface force vector, $N\cdot m^{-2}$; $\boldsymbol{f}$ is volume force vector, $N\cdot m^{-3}$.

Copyright © 2019, the Authors. Published by Atlantis Press.
This is an open access article under the CC BY-NC license (http://creativecommons.org/licenses/by-nc/4.0/).

According to the law of conservation of mass, the fluid mass flowing into the volume is equal to the increment of the fluid mass in the volume, that is[10]

$$-\int_S \rho_w n_w \boldsymbol{n}^{\mathrm{T}} \cdot \boldsymbol{v}_w \mathrm{d}S = \int_V \frac{1}{J}\frac{\mathrm{d}}{\mathrm{d}t}(J\rho_w n_w)\mathrm{d}V \tag{2}$$

In equation (2), the fluid flow through the porous medium obeys the Forchheimer's law[6]

$$sn\boldsymbol{v}_w(1+\beta\sqrt{\boldsymbol{v}_w \cdot \boldsymbol{v}_w}) = -\frac{k_s}{\gamma_w}\mathbf{k}\cdot(\frac{\partial p_w}{\partial \mathbf{x}} - \rho_w \boldsymbol{g}) \tag{3}$$

Where ρ_w is fluid density, kg·m^{-3}; n_w is porosity of the porous medium, dimensionless; $\boldsymbol{v}_w$ is flow velocity (the velocity of fluid flow relative to the solid skeleton), m/s; $\boldsymbol{n}$ is outer normal vector of surface S, dimensionless; J is the ratio of current volume to initial volume of the porous medium, dimensionless; s is saturation, dimensionless; β is fluid flow velocity coefficient, dimensionless; k is permeability coefficient vector, m/s; x is spatial vector, m; g is gravitational acceleration vector, m·s^{-2}.

B. Theoretical Equation of the Fourth Stress Strength

The theory of the fourth stress strength is also known as the theory of distortion energy density, which regards the distortion energy density as the main factor causing the material yield. Its expression is[11, 12]

$$\sqrt{\frac{1}{2}\left[(\sigma_1-\sigma_2)^2+(\sigma_2-\sigma_3)^2+(\sigma_3-\sigma_1)^2\right]} \le [\sigma] \tag{4}$$

Where σ_1, σ_2 and σ_3 are tri-axial principal stresses, Pa; $[\sigma]$ is allowable stress under current operating conditions, Pa.

In this paper, the fourth stress strength theory is applied to the strength check of the casing stress. When the maximum temporal and spacial von Mises stresses satisfy equation (4), it is considered that the casing material meets the safety requirements under the current operating conditions; otherwise, the casing material fails to meet relevant safety requirements, and the casing structure and dimensions need to be modified.

III. NUMERICAL MODEL ESTABLISHED

Fig.1 is a finite element model of underground gas storage established by employing the finite element software ABAQUS and the PYTHON scripting language. The green grid represents the casing, and the orange grid represents the formation. The model was subject to grid division by using hexahedral elements, and a total of 66,396 elements and 100,004 nodes were generated. Formation parameters are shown in Table 1, and casing and cement sheath parameters are shown in Table 2. All data come from an injection-production well of existing gas storage.

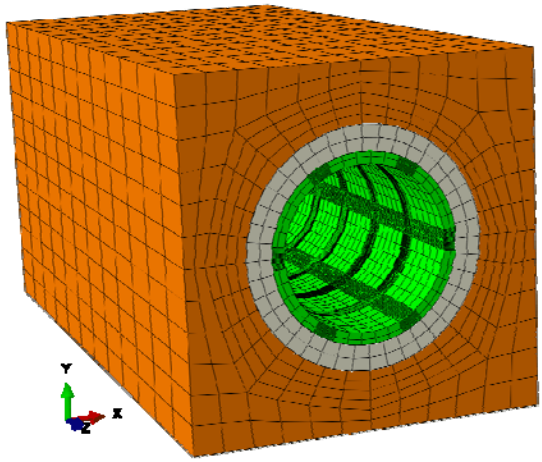

FIGURE I. THE FINITE ELEMENT MODEL OF AN INJECTION-PRODUCTION WELL OF UNDERGROUND GAS STORAGE

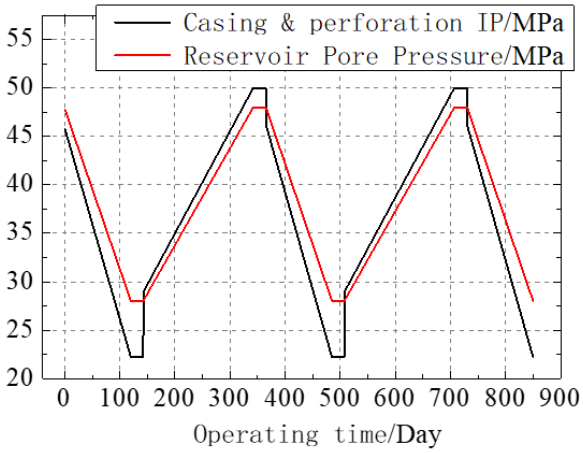

FIGURE II. THE HISTORY OF INTERNAL CASING PRESSURE AND RESERVOIR PORE PRESSURE

TABLE I. FORMATION PARAMETERS

Reservoir depth, m	Vertical (z-axis) principal stress, MPa	Min. horizontal (X-axis) principal stress, MPa	Max. horizontal (Y-axis) principal stress, MPa	Formation pressure, MPa	Formation permeability, mD	Porosity, %	Young modulus, GPa	Poisson ratio
4700	108	84.6	98.7	47.8	2	2.29	35	0.2

TABLE II. CASING AND CEMENT SHEATH PARAMETERS

Young modulus, casing, GPa	Poisson ratio, casing	Casing OD, mm	Casing T, mm	Perforation phase, °	Perforation density, m^{-1}	Perforation D, mm	Young modulus, cement sheath, GPa	Poisson ratio, cement sheath	Cement sheath OD, mm
210	0.3	177.8	9.17	60	16	6	25	0.25	215.95

Fig. 2 shows the history of internal casing pressure and reservoir pore pressure. The downcurve represents gas withdrawal, and the upcurve represents gas injection. At production stage, the reservoir pore pressure is greater than the internal pressures of casing and perforations; at withdrawal stage, the internal pressures of casing and perforations are greater than the reservoir pore pressure, and have sudden change at the time of alternation between injection and withdrawal. 2.5 injection-production cycles were simulated. Data in this figure also come from the same injection-production well of existing gas storage.

IV. SIMULATION RESULTS AND DISCUSSION

Fig. 3 shows the von Mises stress distribution of the model at the end of gas withdrawal. The stress distribution of the whole model is shown on the right, with the local stress detail of perforation shown on the left. It can be seen from the figure that the maximum von Mises stress of the model is located on the inner wall of the perforation in the direction of the minimum horizontal (X-axis) principal stress. The maximum von Mises stress in the figure is 632.1 MPa. The minimum yield strength of the P110 steel casing is 758 MPa. Set the safety coefficient of internal pressure resistance at 1.125, then the allowable stress is $758/1.125 \approx 673.8$ MPa. According to equation (4), 632.1 MPa is less than 673.8 MPa. Therefore, at the end of gas withdrawal, the stress on the casing meets the requirements of safety production.

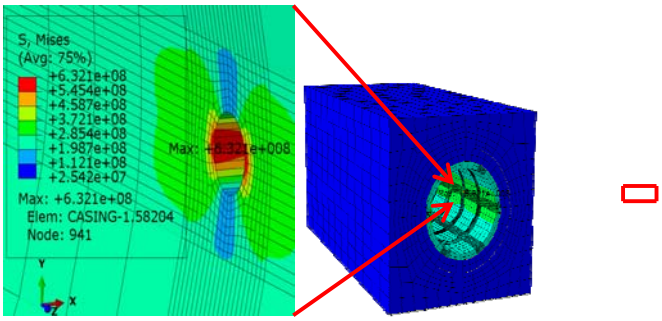

FIGURE III. THE VON MISES STRESS DISTRIBUTION AT THE END OF GAS WITHDRAWAL

Fig. 4 shows the history of the maximum von Mises stress of the casing (located on the inner wall of the perforation) along with the injection-production process. It can be seen from Fig. 4 and Fig. 2 that the maximum von Mises stress of the casing gradually increases in the process of gas withdrawal, gradually decreases in the process of gas injection, and the stress changes suddenly at the alternation between withdrawal and injection. This is because during the operation of the injection-production wells of gas storage, the casing is mainly subjected to the compressional deformation from the virgin rock stress due to the existence of virgin rock formation stress. Therefore, the greater the gas pressure on the inner wall of the casing, the more the virgin rock stress on the casing will be offset, and the less the stress on the casing pipe will be. The maximum spatial von Mises stress of the casing is located on the inner wall of the perforation, and the maximum temporal von Mises stress of the casing occurs at the end of gas withdrawal. Therefore, as long as the von Mises stress on the inner wall of the casing perforation is less than the allowable stress under the operating conditions at the end of withdrawal, it can be concluded that the casing meets the safe production requirements; otherwise, the casing fails to meet relevant safe production requirements. In Fig. 3, the von Mises stress on the inner wall of the casing perforation at the end of withdrawal has been checked. Therefore, the casing stress can meet the safe production requirements in the whole process of production.

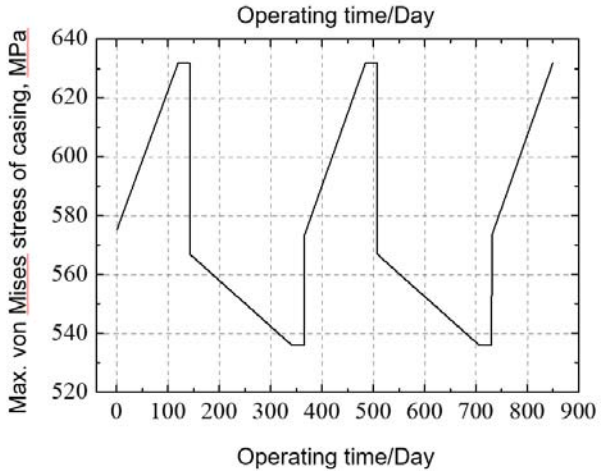

FIGURE IV. THE HISTORY OF THE MAXIMUM VON MISES STRESS OF THE CASING

It is recommended in the literatures[4, 13] that the fatigue damage caused by alternating loads should not be considered before the minimum stress cycle number experienced by the material reaches 10^4 to 10^7. One injection-production cycle of the injection-production well of gas storage lasts for almost one year. For a production period of 30-50 years, there are only dozens of alternating load cycles to be experienced by the casing. Therefore, the impact of material fatigue caused by alternating loads needn't to be considered.

V. MODEL OPTIMIZATION ANALYSIS BASED ON CASING STRESS

It is stated in the proceeding paragraphs that the injection-production process of gas storage has been numerically

simulated, and the casing strength has been checked. Although the safe production requirements are met, the casing structure and dimensions are not necessarily optimal. For different practical situations, how to optimize the casing structure and dimensions while meeting the requirements of safe production remains to be a problem to be solved in the actual production process.

The model above was built by employing the finite element software ABAQUS and the PYTHON scripting language. The whole process of model building was recorded by the PYTHON scripting language. Automatic and parametric modeling can be realized by modifying the model parameters in this script file and inputting it into the PYTHON scripting file. By using this method, one model parameter is modified at a time while the other parameters in the model remain unchanged, and the influence of this parameter on the simulation results can be obtained. By continually modifying the model parameters and conducting comparative analysis, the influence of different parameters on casing stress, and the optimum casing dimensions and structure can be obtained successively. Fig. 5 shows the optimization analysis flow chart of the casing structure and dimensions. Table 3 shows the simulation results of casing stress in the case of vertical wells. Both Table 4 and Table 5 show the calculation results of casing stress in the case of horizontal wells but with different casing axial direction.

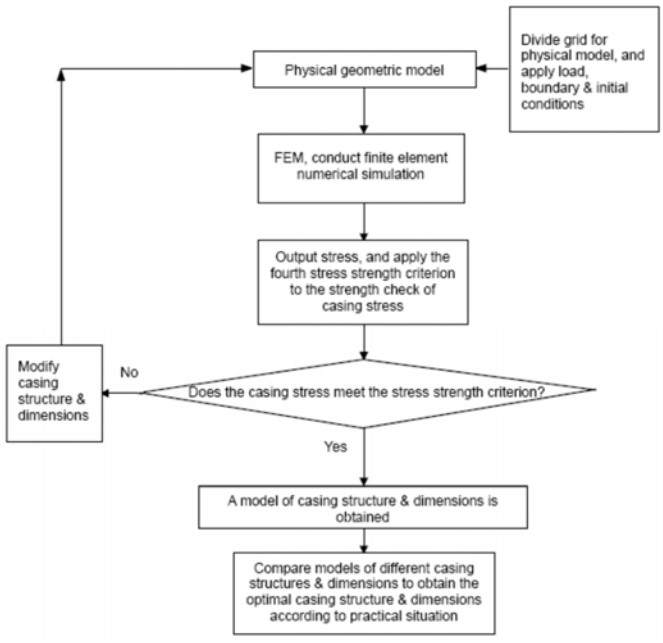

FIGURE V. THE OPTIMIZATION ANALYSIS FLOW CHART OF CASING STRUCTURE AND DIMENSIONS

The initial stress distribution of the formation is $S_V > S_H > S_h$. The value and direction of the formation stress remain unchanged, and the model structure and parameters are the same. The only difference between different operating conditions is that the axial direction of the casing varies. In the case of vertical wells, the casing axis is parallel to the direction of the vertical principal stress S_V. In the case of horizontal wells, the casing axis is parallel to the direction of the maximum or the minimum principal stress as shown respectively in Fig. 4 and Fig. 5.

TABLE III. PARAMETRIC STUDY RESULTS OF CASING STRESS IN THE CASE OF VERTICAL WELLS

Item	Casing T, mm	Perforation D, mm	Phase between the initial perforation and the min. horizontal principal stress, °	Max. von Mises stress of casing at the late stage of withdrawal, MPa	Safe production requirements met or not?
1	7.72	6	0	689.3	No
2	7.72	8.8	0	670.4	Yes
3	7.72	8.8	30	639.6	Yes
4	9.17	6	0	632.1	Yes
5	9.17	6	30	603.0	Yes
6	9.17	8.8	0	616.6	Yes
7	9.17	8.8	10	591.7	Yes
8	9.17	8.8	30	546.3	Yes
9	9.17	8.8	50	587.9	Yes

TABLE IV. PARAMETRIC STUDY RESULTS OF CASING STRESS IN THE CASE OF HORIZONTAL WELLS (THE CASING AXIS IS PARALLEL TO THE DIRECTION OF MAXIMAL HORIZONTAL STRESS)

Item	Casing T, mm	Perforation D, mm	Phase between the initial perforation and the min. horizontal principal stress, °	Max. von Mises stress of casing at the late stage of withdrawal, MPa	Safe production requirements met or not?
1	9.17	6	0	712.0	No
2	9.17	8.8	0	694.9	No
3	9.17	6	30	663.5	Yes
4	9.17	8.8	30	647.3	Yes
5	10.54	6	0	661.3	Yes
6	10.54	8.8	0	646.9	Yes
7	10.54	8.8	10	625.4	Yes
8	10.54	8.8	30	578.3	Yes
9	10.54	8.8	50	621.3	Yes

TABLE V. PARAMETRIC STUDY RESULTS OF CASING STRESS IN THE CASE OF HORIZONTAL WELLS (THE CASING AXIS IS PARALLEL TO THE DIRECTION OF MINIMAL HORIZONTAL STRESS)

Item	Casing T, mm	Perforation D, mm	Phase between the initial perforation and the min. horizontal principal stress, °	Max. von Mises stress of casing at the late stage of withdrawal, MPa	Safe production requirements met or not?
1	9.17	6	0	715.4	No
2	9.17	8.8	0	698.0	No
3	9.17	6	30	696.0	No
4	9.17	8.8	30	679.0	No
5	10.54	6	0	663.6	Yes
6	10.54	8.8	0	649.0	Yes
7	10.54	8.8	10	630.4	Yes
8	10.54	8.8	30	606.4	Yes
9	10.54	8.8	50	626.2	Yes

A comprehensive comparison of Tables 3-5 shows that under the same conditions the von Mises stress increases gradually from Table 3 through Table 5. Thus, it can be concluded that the casing stress is mainly affected by the values of the original bi-axial principal stresses of the formation in the cross section of the casing, while the effect of the original principal stress of the formation in the axial direction of the casing on the casing stress is relatively less. Therefore, for the same formation stress field, in order to minimize the stress on the casing, the original bi-axial principal stress values of the formation in the cross section of the casing should be the two smaller ones among the tri-axial principal stress values. That is to say, in the case of vertical wells as shown in Table 3, the casing axis should be parallel to the direction of the maximum one among the three principal stresses of the formation; in the case of horizontal wells as shown in Table 4, when the casing axis is parallel to the direction of the maximum horizontal principal stress, the casing has the minimum stress.

In the case of vertical wells as shown in Table 3 and horizontal wells as shown in Table 3, the maximum von Mises stress of the casing occurs on the inner wall of the perforation in the direction of the minimum horizontal principal stress S_h; in the case of horizontal wells as shown in Table 5, the maximum von Mises stress of the casing occurs on the inner wall of the perforation in the direction of the maximum horizontal principal stress S_H. To sum up, the maximum von Mises stress of the casing always occurs on the inner wall of the perforation in the direction of the smaller one of the two principal stresses in the cross section of the casing. During spiral perforation completion, perforation in this direction should be avoided. Theoretically, if the perforation in the cross section of the casing deviates 90° from the direction, or perforation is carried out in the direction of the bigger one of the two principal formation stresses in the cross section of the casing, the von Mises stress on the inner wall of the casing perforation is the minimum. Considering the periodicity of spiral perforation which is mostly used in practical perforation programs, the optimal perforation program is to shoot at half the phase angle off this direction in the cross section of the casing (see the last four rows in Tables 3-5).

In Table 4, the stress reduction of item 3 relative to item 1 and item 4 relative to item 2 is approximately 50 MPa; while in Table 5, the corresponding stress reduction is 20 MPa. This indicates that when the difference between the bi-axial principal stresses in the cross section of the casing is relatively great (Table 4), it is more necessary to make perforations off the direction of the smaller one of the two principal stresses in the cross section, which can significantly reduce the von Mises stress on the inner wall of the casing perforation.

It can also be seen from Table 3 through Table 5 that a large diameter perforation can reduce the stress on its inner wall, which is because that a large diameter perforation can mitigate its local stress concentration, making the stress at the perforation approach the average level of the casing pipe. Therefore, large diameter perforation completion should be selected where possible.

REFERENCES

[1] Zhao Zhicheng, Zhu Weiyao, Shan Wenwen, et al. Research on mechanism of solution mining for building underground gas storage in salt cavern [J]. Petroleum Exploration and Development, 2003, 30(5): 107-109. (in Chinese)

[2] Xu Zhenping, Jiang Jianxue, Ge Jingtao, et al. Dynamic numerical simulation of injection-production in depleted reservoir underground gas storage [J]. Natural Gas Exploration & Development, 2011, 34(4): 53-55, 59. (in Chinese)

[3] Ma Huifang. Numerical simulation of Dazhangtuo gas storage [D]. Beijing: China University of Geosciences, 2003. (in Chinese)

[4] Hilbert, L.B., Saraf, V.K. Salt mechanics and casing deformation in solution-mined gas storage operations [R]. ARMA 08-383, 2008.

[5] Chen Weizhong, Wu Guojun, Jia Shanpo. Application of ABAQUS in tunnel and underground engineering [M]. Beijing: China Water Conservancy and Hydropower Press, 2010. (in Chinese)

[6] Zhuang Zhuo, You Xiaochuan, Liao Jianhui, et al. Finite element analysis and application based on ABAQUS [M]. Beijing: Tsinghua University Press, 2009. (in Chinese)

[7] Chen Feng, Yang Chunhe, Bai Shiwei. Investigation on optimized gas recovery velocity of natural gas storage in salt rock layer by numerical simulation [J]. Rock and Soil Mechanics, 2007, 28(1): 57-62. (in Chinese)

[8] Liu Jian, Song Juan, Zhang Fengwei, et al. Safety analysis of casing of gas storage influenced by stochastic factors during operation period [J]. Rock and Soil Mechanics, 2012, 33(12): 3721-3728. (in Chinese)

[9] Zhang Guangming. A numerical simulation study on hydraulic fracturing of horizontal wells [D]. Hefei: University of Science and Technology of China, 2010. (in Chinese)

[10] Zhang G.M., Liu H., Zhang J., et al. Three-dimensional finite element simulation and parametric study for horizontal well hydraulic fracture [J]. Journal of Petroleum Science and Engineering, 2010, 72(3-4): 310-317.

[11] Liu Hongwen. Mechanics of Materials I[M]. Fifth edition. Beijing: Higher Education Press, 2011. (in Chinese)

[12] Guan Zhichuan, Zhao Hongshan. Triaxial prestress design of casing in steam injection wells [J]. Engineering Mechanics, 2007, 24(4): 188-192. (in Chinese)

[13] Liu Hongwen. Mechanics of Materials II[M]. Fifth edition. Beijing: Higher Education Press, 2011. (in Chinese)